

Supplementary Information

for

Peroxymonosulfate activation by Cobalt-doped ferromanganese magnetic oxides through singlet oxygen and radical pathways for efficient sulfadiazine degradation

Fengchun Li ^a, Yawei Gu ^{a,b,*}, Luwei Zhai ^a, Xuan Zhang ^a, Ting Wang ^c, Xia Chen ^a,

Chongqing Xu ^b, Guihuan Yan ^b, Wenqiang Jiang ^{a*}

a. School of Environmental Science and Engineering, Qilu University of Technology

(Shandong Academy of Sciences), Jinan 250353, China.

b. Ecology Institute, Qilu University of Technology (Shandong Academy of Sciences),

Jinan 250103, China.

c. Jinan Eco-environment Monitoring Center of Shandong Province, Jinan 250014,

China

* Corresponding author:

gyw@qlu.edu.cn(Yawei Gu);

jwq@qlu.edu.cn (Wenqiang Jiang)

Text S1. Characteristics of catalyst.

Text S2. EPR analysis.

Text S3. Chemical analysis method

Table S1. Magnetization performance parameters of MFO and CMFO-0.5.

Table S2. Comparison of the reaction parameters with previously reported catalysts for PMS activation.

Table S3. The first-order kinetic reaction rates over MFO, CMFO-0.1, CMFO-0.3, CMFO-0.5 and CMFO-1.0.

Table S4. The first-order kinetic reaction rates of different quenchers.

Table S5. The m/z, molecular formula and structure of SDZ and 13 intermediates.

Fig.S1. SEM images of (a)MFO, (b)CMFO-0.3, and (c) CMFO-1.0.

Fig.S2. Element content map based on EDS data of (a)MFO, (b)CMFO-0.3, and (c) CMFO-1.0.

Fig.S3. FTIR spectra of MFO and CMFO-0.5.

Fig.S4. Zeta potential-pH profiles of CMFO-0.5.

Fig.S5. Leaching concentrations of metal ions at different initial pH values.

Fig.S6. Changes of solution pH during SDZ degradation at different initial pH values.

Fig.S7. Metal leaching of CMFO-0.5 in cycling experiments.

Fig.S8 TGA curves forCMFO-0.4 recorded at 10 °C min⁻¹ heating rate

References.

Text S1. Characteristics of catalyst.

The crystal structure was analysed by X-ray diffraction (XRD) (Rigaku SmartLab SE) in Cu K α radiation (0.1542 nm) at a scan rate of 5 °C min⁻¹ and a scan range of 5° to 90°. X-ray photoelectron spectroscopy (XPS, Thermo Scientific) using Al-k- α radiation (1486.6 eV) was used to measure the metal valence states in the catalyst (before and after the degradation reaction). The BET surface area and mean aperture of the sample were measured by Micromeritics ASAP 2460 instrument. Using a scanning electron microscope (SEM, Sigma 300), the microstructure was examined. Using a Bruker A300, electron paramagnetic resonance (EPR) spectra were acquired to determine the relative strengths of the involved radicals at various points in time. Malvern Zetasizer Nano was used to determine the zero charge pH point (pH_{pzc}) of the catalyst. The magnetic properties of the catalysts were tested with a maximum applied field of 2.17 T at -20 kOe ~ 20 kOe using a vibrating sample magnetometer (VSM) (LakeShore 7404, USA). The electrochemical workstation model CHI 660e was employed to measure electrochemical impedance (EIS) and cyclic voltammetry (CV) curves.

Text S2. EPR analysis.

The active free radicals produced in the CMFO-0.5/PMS system were detected by EPR (Bruker EMXplus-6/1, Germany). The free radicals were captured with two spin trapping agents, 5, 5-dimethyl-1-pyrroline n-oxide (DMPO, > 99%, Macklin) and 2,2,6, 6-tetramethyl-4-piperidol (TEMP, > 99%, Macklin). Prepare 100 mL solution containing 0.2g/L CMFO, add 1mM PMS, take 30 μ L sample, add 30 μ L DMPO(100mM deionized water/methanol as solvent), mix evenly, use a capillary to absorb a certain amount of mixed liquid, and put on a quartz tube. The EPR sample chamber was placed for hydroxyl radical/superoxide radical testing. Take a 30 μ L sample, add 50 μ L TEMP (100mM), mix evenly, absorb a certain amount of the

mixture with a capillary tube, put the quartz tube on, and put it into the EPR sample chamber for testing singlet oxygen free radicals.

Text S3. Chemical analysis method

SDZ was determined by high performance liquid chromatography (LC-10, Shanghai, China) on XDB-C18 (2.1 cm × 4.6 mm, 1.5 μm, Agilent) column connected with an ultraviolet detector. The mobile phase is acetonitrile: water (0.1% formic acid) 3:7, (v/v). The injection volume was 20 μL and the flow rate was 1 mL/min. The column temperature was 25°C. The detection wavelength is 270 nm.

An ultraviolet-visible spectrophotometer (UV-1810, Beijing Puxi general instrument, China) was used to measure the change of PMS concentration during SDZ degradation at 735 nm wavelength. The leaching concentrations of Co, Mn and Fe ions during SDZ degradation were determined by inductively coupled plasma optical spectroscopy (Thermo Scientific iCAP 7000 Series, UK). The possible intermediates in the degradation process of SDZ were identified by liquid chromatography-mass spectrometry (LC-MS, LS-1290UPLC, MS Agilent Qtof6550). The total organic carbon (TOC) of the reaction system was determined using a TOC analyzer (Shimadzu, Japan).

Table S1. Magnetization performance parameters of MFO and CMFO-0.5.

Catalyst	Coercivity (H_c)	Saturation Magnetization (M_s)	Remanent Magnetization (M_r)
MFO	32.9414	21.8742	1.9689
CMFO-0.5	1236.99	32.8440	14.6013

Table S2. Comparison of the reaction parameters with previously reported catalysts for PMS activation.

Pollution	Catalysts loading	PMS dosage	Removal efficiency	k	Ref
BPA (10 mg L ⁻¹)	Mn _{1.8} Fe _{1.2} O ₄ (0.1 g L ⁻¹)	0.2 g L ⁻¹	95% (30 min)	0.102 min ⁻¹	1
Phenol (20 mg L ⁻¹)	LaCo _{0.4} Cu _{0.6} O ₃ (0.1 g L ⁻¹)	0.2 g L ⁻¹	100% (12 min)	0.302 min ⁻¹	2
SMZ(0.18 mM)	CuCo ₂ O ₄ (0.1 g L ⁻¹)	1mM	100% (30 min)	0.141 min ⁻¹	3
SDZ (20 μM)	Fe ₃ O ₄ -Mn ₃ O ₄ (0.1 g L ⁻¹)	0.8mM	100% (20 min)	0.210 min ⁻¹	4
SDZ (10 mg L ⁻¹)	MnFe ₂ O ₄ /δ-MnO ₂ (1:4) (0.2 g L ⁻¹)	2 mM	~100 % (30 min)	0.139 min ⁻¹	5
SDZ (20 mg L ⁻¹)	CMFO-0.5 (0.2 g L ⁻¹)	1mM	100% (10 min)	0.491 min ⁻¹	Our work

To assess the efficacy of catalysts in the degradation of SDZ, the kinetics of SDZ degradation were analyzed using quasi-primary modes. The degradation rate constant (k_{obs}) equation (1) was then determined by linear regression analysis of the aforementioned equation.

$$\ln(C_t/C_0) = -k_{obs}t \quad \#(1)$$

where C_0 and C_t are the initial SDZ concentration and the concentration of SDZ at a certain reaction time t , respectively. The high value of the regression coefficient ($R^2 =$

0.9952) (as shown in **Table S3**) indicates that the SDZ degradation kinetics can be well-fitted by first-order kinetics.

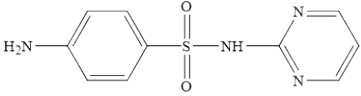
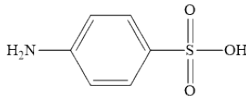
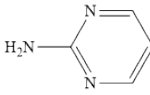
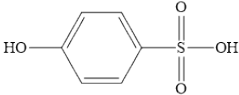
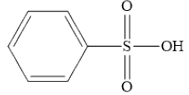
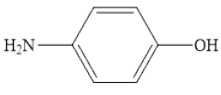
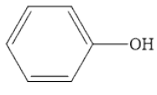
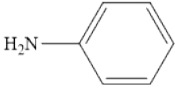
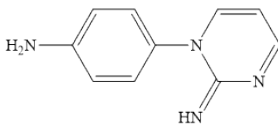
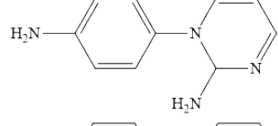
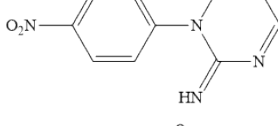
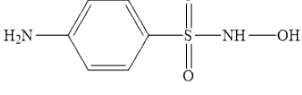
Table S3. The first-order kinetic reaction rates over MFO, CMFO-0.1, CMFO-0.3, CMFO-0.5 and CMFO-1.0. Reaction conditions: [CMFO] = 0.2 g L⁻¹, [PMS] = 1 mM, [SDZ] = 20 mg L⁻¹ and pH = 5.6.

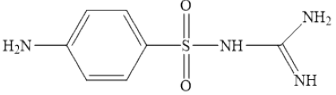
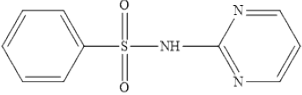
Catalysts	k (min ⁻¹)	R ²
MFO	0.02	0.9271
CMFO-0.1	0.13	0.9480
CMFO-0.3	0.48	0.9571
CMFO-0.5	2.40	0.9162

Table S4. The first-order kinetic reaction rates of different quenchers. Reaction conditions: [CMFO] = 0.2 g L⁻¹, [PMS] = 1 mM, [SDZ] = 20 mg L⁻¹ and pH = 5.6.

Condition	k (min ⁻¹)	R ²
No quencher	0.4094	0.9928
50 mM EtOH	0.0574	0.8791
100 mM EtOH	0.0402	0.8639
50 mM TBA	0.2938	0.9562
100 mM TBA	0.2178	0.9948
5 mM FFA	0.0141	0.9033
5 mM BQ	0.1551	0.9971

Table S5. The m/z, molecular formula and structure of SDZ and 13 intermediates.

Compounds	[M+H] ⁺ m/z	Molecular formula	Molecular structure
SDZ	251	C ₁₀ H ₁₀ N ₄ SO ₂	
P1	173	C ₆ H ₇ NSO ₃	
P2	96	C ₄ H ₅ N ₃	
P3	174	C ₆ H ₆ SO ₄	
P4	158	C ₆ H ₆ SO ₃	
P5	109	C ₆ H ₃ NO	
P6	95	C ₆ H ₅ OH	
P7	93	C ₆ H ₇ N	
P8	186	C ₁₀ H ₁₀ N ₄	
P9	187	C ₁₀ H ₁₁ N ₄	
P10	217	C ₁₀ H ₈ N ₄ O ₂	
P11	188	C ₆ H ₈ N ₂ SO ₃	

P12	215	$C_7H_{11}N_3SO_2$	
P13	235	$C_{10}H_9N_3SO_2$	

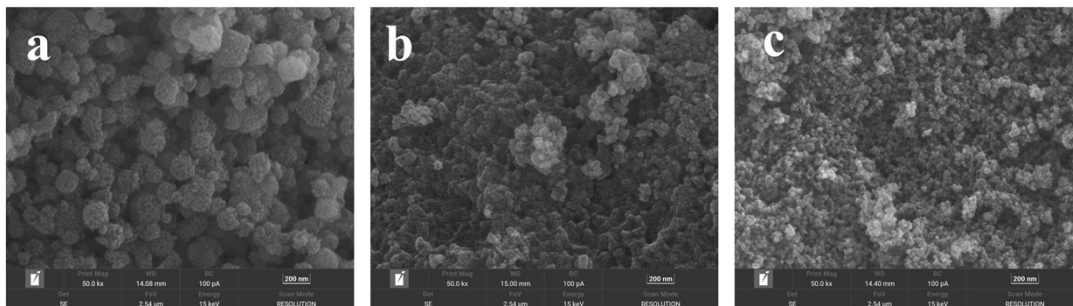


Fig.S1. SEM images of (a)MFO, (b)CMFO-0.3, and (c) CMFO-0.5.

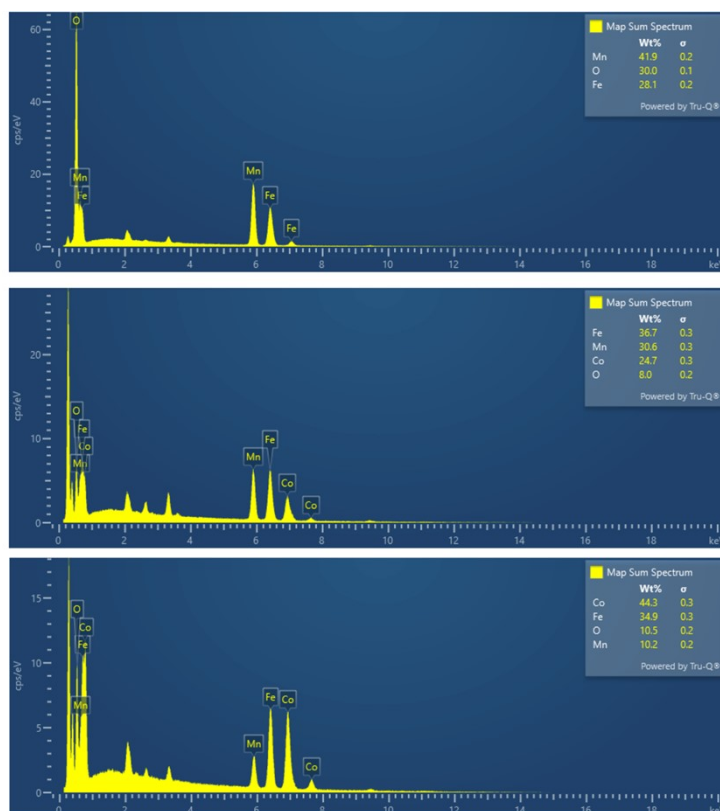


Fig.S2. Element content map based on EDS data of (a)MFO, (b)CMFO-0.3, and (c) CMFO-1.0.

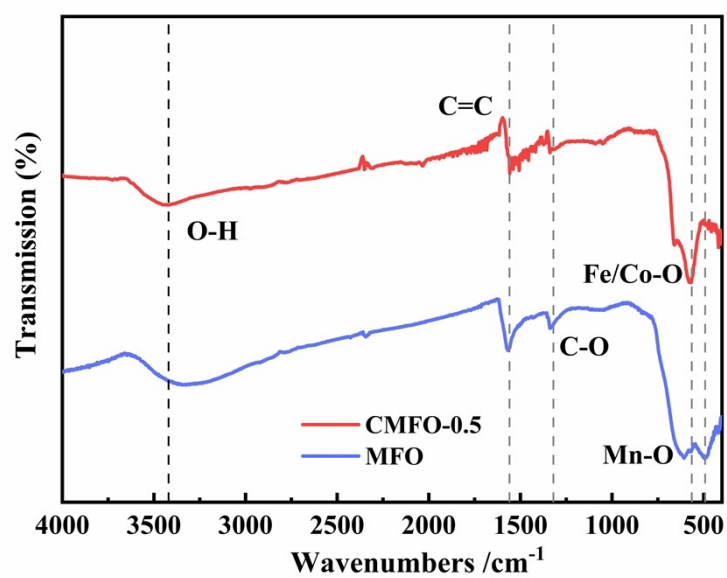


Fig.S3. FTIR spectra of MFO and CMFO-0.5.

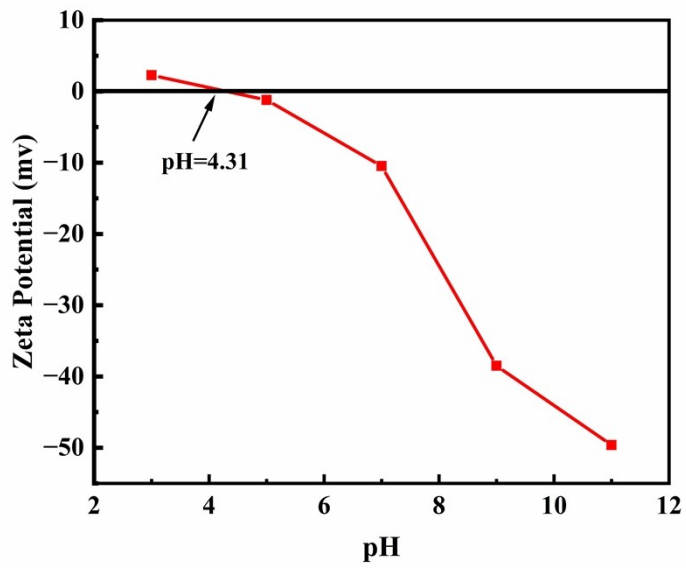


Fig.S4. Zeta potential-pH profiles of CMFO-0.5.

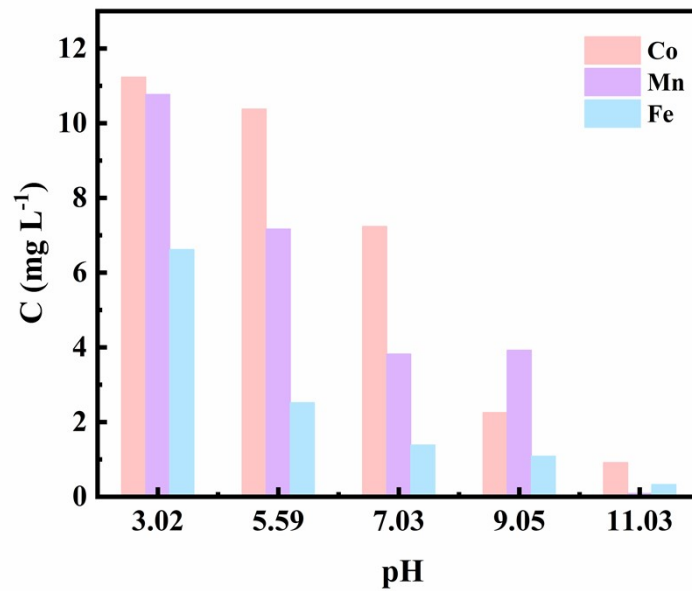


Fig.S5. Leaching concentrations of metal ions at different initial pH values.

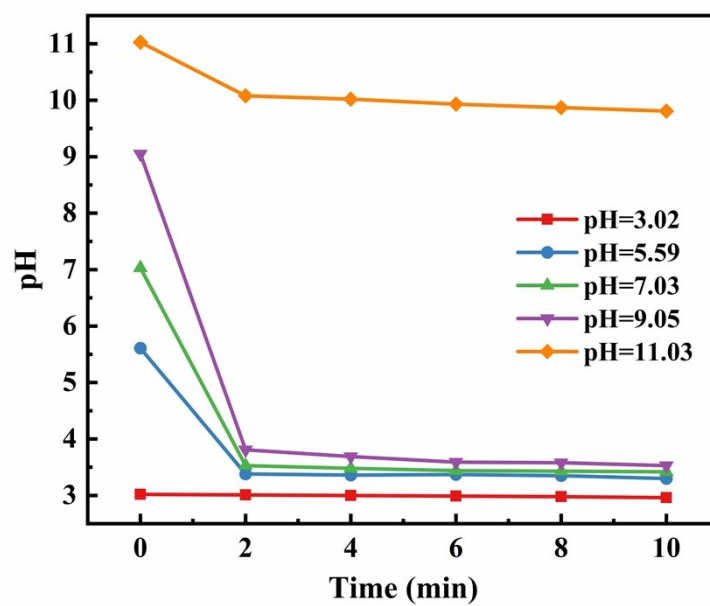


Fig.S6. Changes of solution pH during SDZ degradation at different initial pH values.

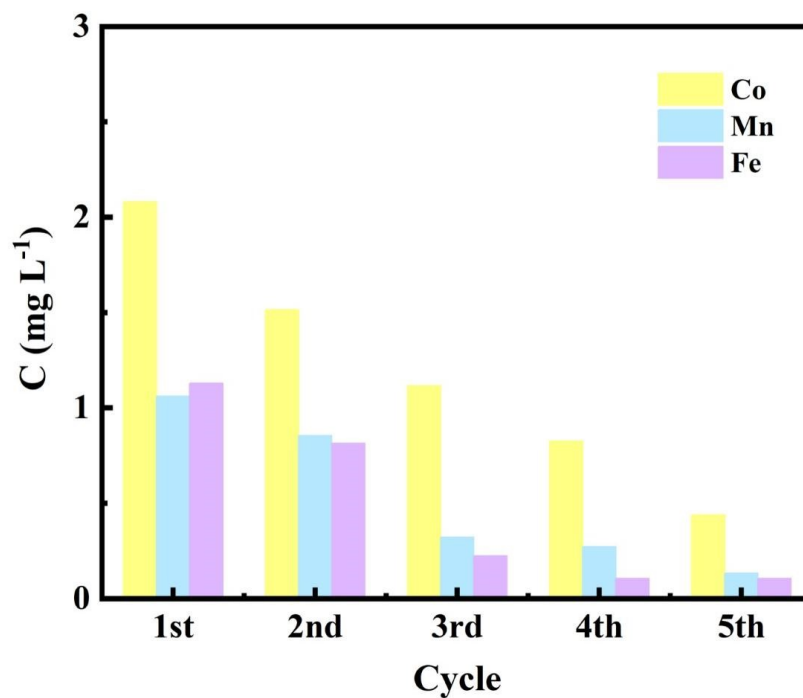


Fig.S7. Metal leaching of CMFO-0.5 in cycling experiments.

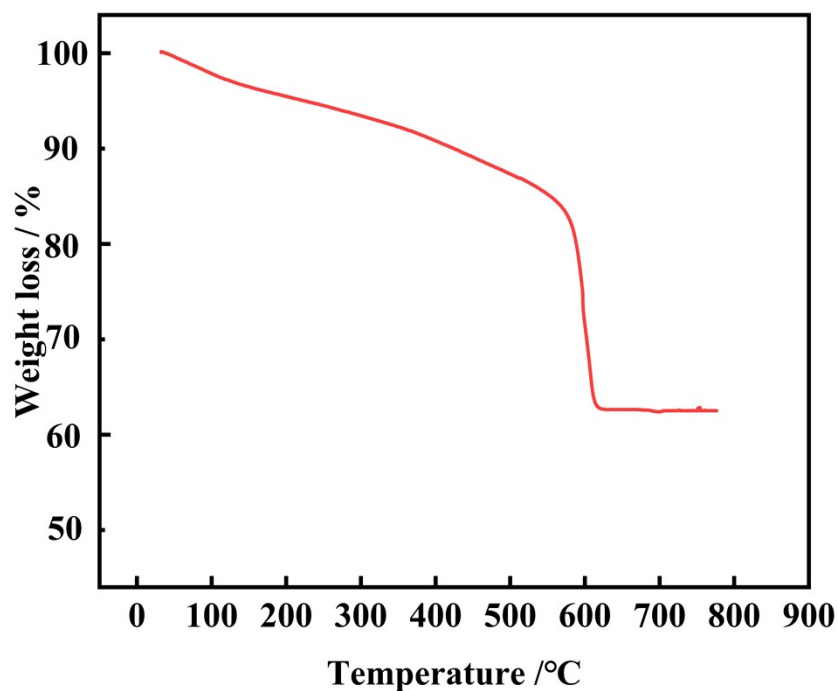


Fig.S8 TGA curves for CMFO-0.4 recorded at 10 °C min⁻¹ heating rate

References

1. G.-X. Huang, C.-Y. Wang, C.-W. Yang, P.-C. Guo and H.-Q. Yu, *Environ. Sci. Technol.*, 2017, **51**, 12611-12618.
2. S. Lu, G. Wang, S. Chen, H. Yu, F. Ye and X. Quan, *J. Hazard. Mater.*, 2018, **353**, 401-409.
3. C. Chen, L. Liu, Y. Li, W. Li, L. Zhou, Y. Lan and Y. Li, *Chem. Eng. J.*, 2020, **384**.
4. J. Chen, K. Chu, S. Sun, H. Chen, B. Song, J. Wang, Z. Liu and L. Zhu, *Journal of Environmental Chemical Engineering*, 2023, **11**.
5. L. Zhu, Z. Shi, L. Deng and Y. Duan, *Colloids Surf. Physicochem. Eng. Aspects*, 2021, **609**.